Experimental investigation of novel powder bed friction stir process for AZ31B Mg alloy

Prabhakar Kumar Singh, Akash Mukhopadhyay, Probir Saha*

Indian Institute of Technology Patna, Bihta, Patna, Bihar, India

Presented in International Conference on Precision, Micro, Meso and Nano Engineering (COPEN - 12: 2022)
December 8th - 10th, 2022 IIT Kanpur, India

ABSTRACT

The current work focused on the process response and mechanical properties variation of the AZ31B powder deposit made by an in-house developed process at a laboratory scale named Powder Bed Friction Stir (PBFS). The PBFS process employs friction stirring as a heating source instead of a laser or electron beam, as in powder bed fusion. Despite the tremendous effectiveness of Mg alloys for structural applications, a suitable route is still being searched for. The motivation of the current work is to explore the potential of the newly developed PBFS process for AZ31B Mg alloy deposition. With 1200rpm and 360 mm/min, the experimentation was carried out using the CPF tool to make a 7mm thick deposit on the AZ31B Mg plate. The process response and mechanical properties were studied to compare the result with wrought Mg alloy.

KEYWORDS

Powder Based Process,
Additive Manufacturing,
Mg Alloy,
Temperature,
Mechanical Properties.

1. Introduction

Due to the excellent strength-to-weight ratio and many unique physical and chemical properties, Magnesium alloys have found wide-scale applications in various sectors, such as automobile, electronic, aerospace, and biomedical (Blawert et al., 2004; Joshi et al., 2022; Xu et al., 2019). Although having so much effectiveness as the lightest structural material, magnesium alloys have been explored less due to their inherent limitations (Liu et al., 2008; Mukai et al., 2001). However, these limitations can be addressed either with the development of Mg alloy or a potential processing route to enhance its formability, surface performance, and bulk properties (Mukai et al., 2001; Song, 2013).

As a critical factor in addressing the inherited limitation with Mg alloys is processing routes, solid-state additive manufacturing (AM) such as AFS-D could be advantageous since fusion-based additive manufacturing processes possess defects like grain coarsening and thermal stress (Mukhopadhyay & Saha, 2020).

The advantages of using solid-state AM were seen in many studies. Kandasamy et al. (2013) used this solid-state AM process AFS-D for depositing a solid feed rod of AZ31-H24 magnesium alloy and powder WE43 onto the substrates. They found that the process could consolidate and deposit magnesium powder into a fully dense, defect-free, wrought-free structure with desirable properties. In a similar experiment with WE43, Calvert et al. (2015) discovered excellent inter-layer mixing between deposited layers using powder and solid filler rods.

The literature has picturized powder's potential use for fully dense functionally graded material fabrication. However, powder passage through a hollow tool during AFSD leads to tool-hole clogging (Chaudhary et al., 2022a). Also, prerequisites for feedstock making from powder and auxiliary feedstock pushing mechanisms during AFS-D hinder its extent as a processing route (Calvert et al., 2015; Mukhopadhyay & Saha, 2020). Chaudhary et al. (2022b) used an external powder feeding to address the issue and found a good consolidation. Nevertheless, the build height was not sufficient.

So, the current work is focused on the experimental investigation of the AZ31B deposit made with external powder feeding. An in-house process named Powder Bed Friction Stir (PBFS) is developed to facilitate the experimentation, inspired by the primary mechanism of powder bed fusion, where no additional setting is required for feedstock pushing; instead, a powder bed

*Corresponding author E-mail: psaha@iitp.ac.in

https://doi.org/10.58368/MTT.22.1.2023.57-62

is used. The Powder Bed Friction Stir (PBFS), introduced in the author's other work, employs friction stirring as a heating source instead of a laser or electron beam, as in powder bed fusion.

The current work aims to see the process response and mechanical properties variation observed in AZ31B deposits made by external powder feeding using an in-house developed process, PBFS.

2. Materials and Methods

Initially, as-received AZ31B Mg alloy powder was analyzed for composition (refer to Fig. 1(d)). The average powder particle size of 112±12 µm was used in the PBFS process onto the AZ31B Mg alloy plate. The plate, having dimensions 200*200*10 mm, was fixed onto the SS310 backing plate with D2 die steel mold to generate enough pressure and to keep the powder in the desired shape. The schematics, actual setup photograph, and fixture arrangement are shown in Fig.1 (b), 1 (c), and 1 (d), respectively.

Since no existing literature was found for the PBFS process with AZ31 Mg alloy powder, appropriate process inputs, viz. tool design, traverse speed (v), and spindle speed (ω), were identified through experimentation, reported in the authors' other work. The PBFS process was started with a plain shoulder tool (PST) of shoulder diameter 32 mm with two sets of ω/v (1200/360 and 900/200) ratios. However, the deposition consisted of defects. The tool design significantly influenced the deposition rate and was discussed in the author's other work. It was observed that the Circular protruded feature (CPF) contributed to successful deposition. The 3D CAD model of the tool was made using Creo software and is shown in Fig. 2.

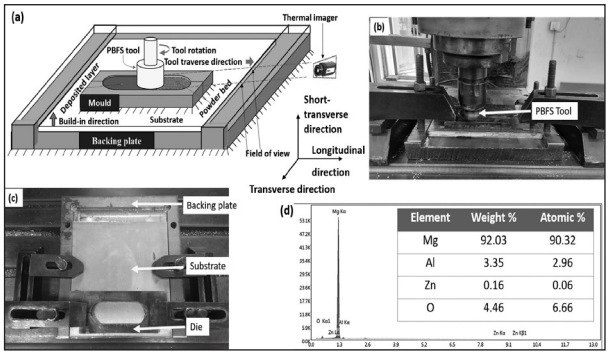

Fig. 1. Showing (a) Schematic of PBFS process with thermal measurement;
(b) actual photographs of PBFS setup;
(c) plate and mold arrangement;
(d) compositional analysis of the AZ31B powder.

At the initial stages of PBFS, we started with preheating the substrate using the to- and fro motion of the tool. Once enough temperature was observed, the powder was poured into the stirring zone, and the tool was raised by the intended layer thickness (0.2mm). A single layer was deposited while the tool completed one cycle of its traverse motion. While going with a single pass, we noticed excessive flashes on a single side, so we started with a double pass in a single layer to minimize the flash. The same cycle was repeated 35 times to deposit a height of 7mm.

The temperature was monitored during PBFS by an infrared thermal imager (A655sc; FLIR) (Fig. 1(a)) placed at approximately 800 mm via maintaining the focus on the tool. The emissivity was calibrated before the experimentation using a previously made AZ31B deposit and hot plate (10-MLH; REMI). With an increment of 50° C/ step, an infrared thermal imager measured

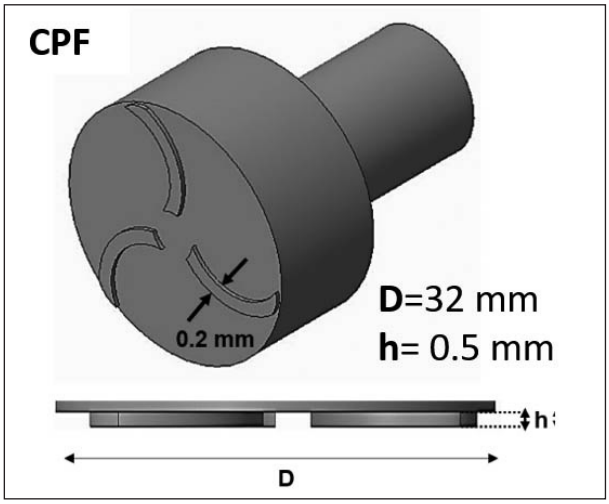

Fig. 2. 3D CAD model of PBFS tool

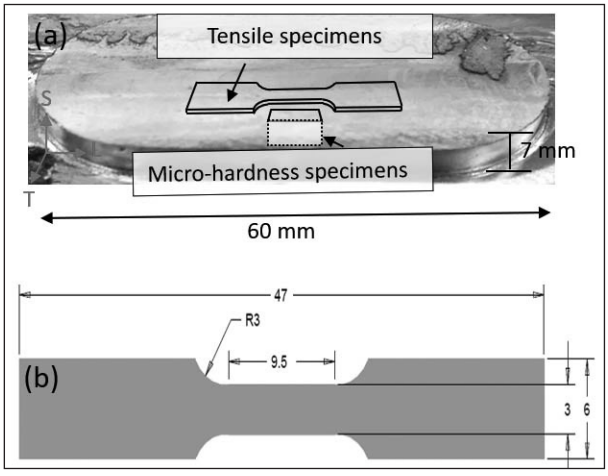

Fig. 3. Showing (a) Reference location in the deposit for tensile and micro-hardness specimens;
(b) schematics of tensile sample.

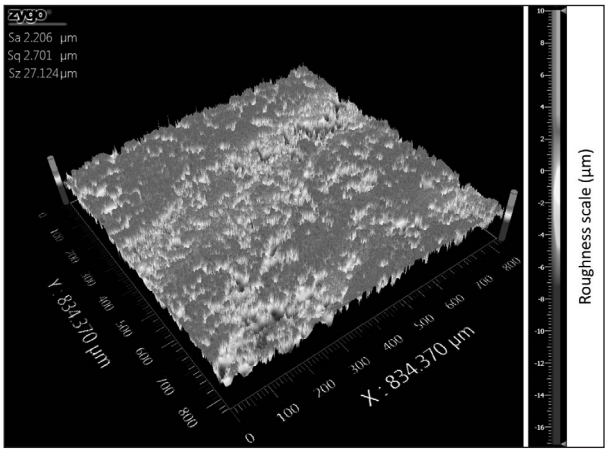

Fig. 4. Showing the average surface roughness value of the deposit.

the corresponding change in the deposit's temperature. The calibrated emissivity was found to be 0.69. A preliminary test of the AZ31B deposit was started with visual inspection using a surface profilometer (Zygo; ZeGage). The miniature specimens (refer to 3(a), (b)) in the longitudinal direction were cut using a W-EDM machine (Electronica; SPRINTCUT) to perform the tensile test on a universal tensile testing machine (ZWICK/ROELL; Z050). The samples were taken from the deposit's top, middle, and bottom sections. The quasi-static testing was performed with a 2 kN load and 0.001/s strain rate, and the broken sample underwent fractography analysis in Field Emission Scanning Electron Microscope (HITACHI; S4800). Vicker's Microhardness was also measured at the position marked in Fig. 3(a) in a micro-hardness testing machine (ZHµ/ST2000; Zwick/Roell) with a normal load of 100 gf for the top, middle and bottom sections. Along three vertical lines, 27 indents were marked for measuring Microhardness. By making a cluster of three readings, a single average value was calculated vertically in each section. Later these values are averaged horizontally to get a single value on the top, middle and bottom sections.

3. Results and Discussion

A successful AZ31B powder deposition onto the substrate using PBFS lays out the initial step in comprehending the surface quality and section-wise analysis. Further, the study of the temperature and section-wise mechanical properties variation theorizes the result. Later, successfully deposited AZ31B powder using PBFS was analyzed for porosity and fractography.

3.1. Surface morphology

The analysis begins with a visual inspection of a freshly made deposit using a surface profilometer. The overall height of the deposit was 6.8 mm instead of 7 mm, as expected. This reduction in layer thickness may be due to an onion ring pattern, which can be related to advance per revolution (APR). During the deformation, some material comes out of the deposition zone. It forms the onion skin pattern due to simultaneous rotational and translational motion that alters the surface roughness. The average surface roughness value found was 2.206 µm, shown in Fig. 4.

3.2. Porosity

After visual inspection, porosity in the deposit was found and calculated using Eq. (1) (Mukhopadhyay & Saha, 2020).

$$\rho p = \left(1 - \frac{\rho d}{\rho}\right) \times 100\% \quad \text{.....(1)}$$

Where ρ_p and ρ_d are the porosity and bulk density of the deposit, respectively, and ρ is the bulk density of the magnesium alloy.

The value of porosity percentage was found to be 4.6 %, attributed to insufficient pressure applied with the tool onto the substrate and powder particle or improper selection of process inputs. We currently work on the provision by which porosity issues could be addressed.

3.3. Thermal response

Mg alloy powder is prone to catching fire because of its pyrophoric nature. One of the purposes of temperature measurement is the avoidance of such incidence. The field of view of the thermal imaging camera was adjusted and set for measuring the temperature during the process (refer to Fig 5(a)). The experimentation started with preheating, contributing to the first layer's temperature with the contribution from the plastic deformation of the powder material and the frictional heat generated at the tool/powder material interface against the substrate. Moreover, the formerly deposited layer acted as a build surface for the subsequent layers. The rise in the Tpeak can be seen in Fig. 5(b), where the temperature in the bottom, middle and top sections were 421°C, 440°C, and 455°C, respectively. Also, Tpeak for the ω;1200 rpm and v;360 mm/

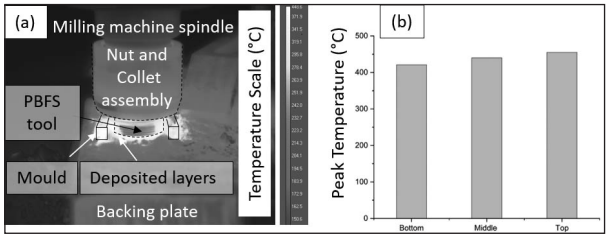

Fig. 5. Showing (a) field of view of thermal imagine camera; (b) section-wise peak temperature.

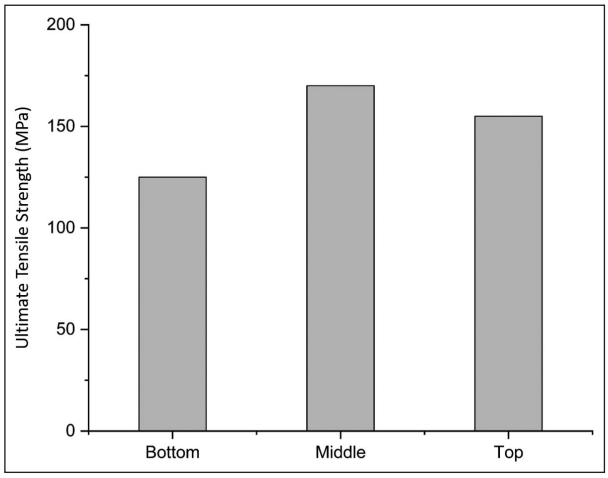

Fig. 6. Section-wise UTS values

min was calculated using Arbegast and Hartley's equation mentioned below (Commin et al., 2009);

$$\frac{Tpeak}{Tm} = k\left(\frac{\omega^2}{V\times 10^4}\right)^{\alpha} \quad \text{.....(2)}$$

Where T_m is the melting temperature of AZ31B (610°C), ω (rpm), and v (mm/s) is the tool's rotational and welding speeds used during PBFS. k and α are constants as 0.8052 and 0.0442, respectively (Commin et al., 2009).

3.4. Mechanical characterization

Material characterization comprised tensile test and micro-hardness of the top, middle, and bottom sections of the PBFS bulk deposition.

The decrease in the AZ31B deposit's ultimate tensile strength (UTS) value compared with AZ31B wrought magnesium alloy is likely due to the initial material condition, where the AZ31B powder was used for bulk deposition. Also, PBFS is a thermomechanical process that results in high heat and a significant temperature value, which would have facilitated annealing over dislocation pileups. The section-wise UTS value of the deposition is shown in Fig. 6, which is comparable. The UTS values for the bottom, middle, and top sections were 125MPa, 170MPa, and 155MPa, respectively. The different UTS values of the top, middle and bottom sections could be because of grain refinement and recrystallization that occurred during the process, which is the inherent characteristic of the PBFS process. The re-stirring action affects layers beneath the shoulder end surface to a depth of 2.5 mm- 3.5 mm, which helps the middle layer undergo significant recrystallization than the other two layers (Mason et al., 2021). Also, the bottom layer would have experienced annealing. Additionally, the porosity present in the subsequent layers alters the overall UTS.

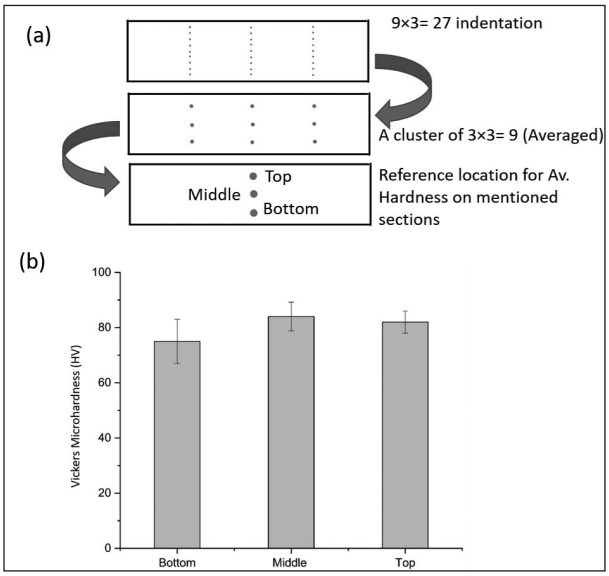

Fig. 7. Showing (a) reference position for indent on deposit in the transverse direction; (b) micro-hardness variation in different sections.

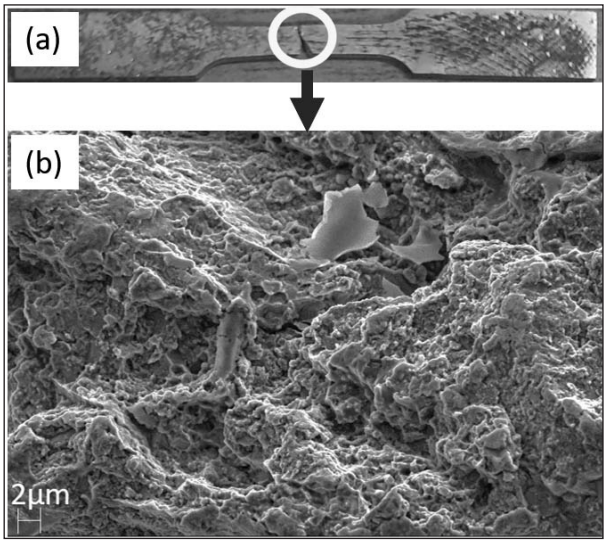

Fig. 8. (a) Broken sample; (b) fractography image.

Microhardness of PBFS deposition was measured with Vickers Hardness (Hv) tests at the position

marked in Fig. 7(a) and compared with wrought magnesium alloy. The deposit's increased hardness values indicate the presence of uniformly distributed intermetallic compounds (IMCs) within the bulk deposition region. The obtained microhardness values in the bottom, middle, and top sections were 75±8.02 Hv, 84±5.2 Hv, and 82±4.04 Hv, respectively. The hardness variation within the layers is because of the extent of recrystallization and annealing. Substantial recrystallization in the middle layer and significant annealing in the bottom layer resulted in such hardness shown in Fig. 7(b).

3.5. Fractography

The fractography analysis was done with a broken sample of the tensile test. Since the middle layer showed higher strength, we examined it to understate the failure mechanisms. The region in the fracture surface of the PBFS tensile sample shows the presence of cups, dimples, and microvoid coalescence (refer to Fig. 8(b)).

4. Conclusion

The PBFS process was successfully established for deposition from Mg alloy powder AZ31B. However, different characteristics were observed in the fabricated deposit for different sections (Top, Middle, and Bottom).

- The deposit's top surface was characterized by onion skin, and the average surface roughness was 2.206 µm.
- Examination showed some amount of porosity (4.6%)in the deposit due to insufficient pressure resulting in a lower UTS.
- The process response in the form of temperature was measured across layers. Accumulating heat with time led to a higher Tpeak in the Top and Middle layers compared to the Bottom layers.
- The middle layers underwent recrystallization due to re-stirring, which led to an increment in UTS. However, the bottom layers faced annealing action and exhibited less UTS. These observations also fit well with the temperature variation.
- Hardness values decreased towards the bottom due to the decreasing temperature trend preventing the formation of IMCs.
- Fractographic analysis revealed a ductile failure mode evidenced by dimples, cups, etc.

References

Blawert, C., Hort, N., & Kainer, K. U. (2004). Automotive applications of magnesium alloys. *Materials Science Forum*, *419–422*(I), 67–72. https://doi.org/10.4028/www.scientific.net/msf.419-422.67

Calvert, J. R., Reynolds, W. T., & Williams, C. B. (2015). *Microstructure and mechanical properties of WE43 alloy produced via additive friction stir technology*.

Chaudhary, B., Jain, N. K., & Murugesan, J. (2022a). Development of friction stir powder deposition process for repairing of aerospace-grade aluminum alloys. *CIRP Journal of Manufacturing Science and Technology*, *38*, 252–267. https://doi.org/10.1016/j.cirpj.2022.04.016

Chaudhary, B., Jain, N. K., & Murugesan, J. (2022b). Experimental investigation and parametric optimization of friction stir powder additive manufacturing process for aerospace-grade Al alloy. *International Journal of Advanced Manufacturing Technology*, *123*(1–2), 603–625. https://doi.org/10.1007/s00170-022-10211-5

Commin, L., Dumont, M., Masse, J. E., & Barrallier, L. (2009). Friction stir welding of AZ31 magnesium alloy rolled sheets: Influence of processing parameters. *Acta Materialia*, *57*(2), 326–334. https://doi.org/10.1016/j.actamat.2008.09.011

Joshi, S. S., Patil, S. M., Mazumder, S., Sharma, S., Riley, D. A., Dowden, S., Banerjee, R., & Dahotre, N. B. (2022). Additive friction stir deposition of AZ31B magnesium alloy. *Journal of Magnesium and Alloys*, *xxxx*. https://doi.org/10.1016/j.jma.2022.03.011

Kandasamy, K., Renaghan, L. E., Calvert, J. R., Creehan, K. D., & Schultz, J. P. (2013). Solid-state additive manufacturing of aluminum and magnesium alloys. *Materials Science and Technology*.

Liu, M., Qiu, D., Zhao, M. C., Song, G., & Atrens, A. (2008). The effect of crystallographic orientation on the active corrosion of pure magnesium. *Scripta Materialia*, *58*(5), 421–424. https://doi.org/10.1016/j.scriptamat.2007.10.027

Mason, C. J. T., Rodriguez, R. I., Avery, D. Z., Phillips, B. J., Bernarding, B. P., Williams, M. B., Cobbs, S. D., Jordon, J. B., & Allison, P. G. (2021). Process-structure-property relations for as-deposited solid-state additively manufactured high-strength aluminum alloy. *Additive Mnf*, *40*. https://doi.org/10.1016/j.addma.2021.101879

Mukai, T., Yamanoi, M., Watanabe, H., & Higashi, K. (2001). Ductility enhancement in AZ31 magnesium alloy by controlling its grain structure. *Scripta Materialia*, *45*(1), 89–94. https://doi.org/10.1016/S1359-6462(01)00996-4

Mukhopadhyay, A., & Saha, P. (2020). Mechanical and microstructural characterization of aluminium powder deposit made by friction stir based additive manufacturing. *Journal of Materials Processing Technology*, *281*. https://doi.org/10.1016/j.jmatprotec.2020.116648

Song, G. L. (2013). Corrosion behavior and prevention strategies for magnesium (Mg) alloys. In *Corrosion Prevention of Magnesium Alloys: A volume in Woodhead Publishing Series in Metals and Surface Engineering* (pp. 3–37). Elsevier Ltd. https://doi.org/10.1533/9780857098962.1.3

Xu, T., Yang, Y., Peng, X., Song, J., & Pan, F. (2019). Overview of advancement and development trend on magnesium alloy. *Journal of Magnesium and Alloys*, *7*(3), 536–544. https://doi.org/10.1016/j.jma.2019.08.001

Prabhakar Kumar Singh is pursuing doctoral research in the Department of Mechanical Engineering, Indian Institute of Technology Patna (IIT-P), India. He attended the National Institute of Foundry and Forge Technology (NIFFT), India, for his M.Tech program. He received his bachelor's degree (B.E.) in Mechanical Engineering from Birsa Institute of Technology (BIT), Sindri, India. His current research topic is "Fabricating 3D structures with AZ31B powder using solid-state additive manufacturing". His area of expertise is solid-state additive manufacturing and mechanical microstructural characterization.
(E-mail: prabhakar_1921me14@iitp.ac.in)

Akash Mukhopadhyay is currently pursuing his Ph.D at the Department of Mechanical Engineering, Indian Institute of Technology Patna in the specialization 'Manufacturing'. Before joining his Ph.D., he received B.E. in Production Engineering from Jadavpur University and M.Tech. degree in Mechanical Engineering (discipline: Manufacturing) from the National Institute of Technology Rourkela. He is doing active research in materials characterization in a project on the friction-stirring-based additive manufacturing process. His other work includes conventional machining, optimization, friction stir welding, etc. He has published three journal papers, three conference papers, and one book chapter from his research work.
(E-mail: akash.pme16@iitp.ac.in)

Dr. Probir Saha is currently working as a Head and Associate Professor in the Department of Mechanical Engineering, IIT Patna. He obtained his Ph.D in 2009 from IIT Kharagpur, M.Tech from IIT Delhi in 2002, and B.E from Jadavpur University in 2001. He has already guided three Ph.D students who have got opportunities from IIT and foreign universities in faculty and postdoctoral positions. Five more Ph.D students are presently working under his supervision. He is currently doing active research on micro-EDM, micro-EDG, and micro-FSW. His other research includes AFS-D. He is also working on several projects funded by different agencies.